https://doi.org/10.5194/amt-2022-147
Preprint. Discussion started: 28 June 2022

Atmospheric Measurement Techniques Discussions

Realtime measurement of phase partitioning of organic compounds using a Proton-Transfer-Reaction Time-of-Flight Mass Spectrometer coupled to a CHARON inlet

Yarong Peng[1,2], Hongli Wang[2,*], Yaqin Gao[2], Shengao Jing[2], Shuhui Zhu[2], Dandan Huang[2], Peizhi Hao[3], Shengrong Lou[2], Tiantao Cheng[4,5,*], Cheng Huang[2], Xuan Zhang[3,*]

[1] Department of Environmental Science and Engineering, Fudan University, Shanghai, 200438, China

[2] State Environmental Protection Key Laboratory of Formation and Prevention of Urban Air Pollution Complex, Shanghai Academy of Environmental Sciences, Shanghai, 200233, China

[3] School of Natural Sciences, University of California, Merced, 95343, USA

[4] Department of Atmospheric and Oceanic Sciences, Fudan University, Shanghai, 200438, China

[5] Big Data Institute for Carbon Emission and Environmental Pollution, Fudan University, Shanghai, 200438, China

Correspondence to: Hongli Wang (wanghl@saes.sh.cn), Tiantao Cheng (ttcheng@fudan.edu.cn), Xuan Zhang (xzhang87@ucmerced.edu)

https://doi.org/10.5194/amt-2022-147
Preprint. Discussion started: 28 June 2022


Atmospheric Measurement Techniques Discussions

Abstract. Understanding the gas-particle partitioning of semivolatile organic compounds (SVOCs) is of crucial importance in the accurate representation of the global budget of atmospheric organic aerosols. In this study, we quantified the gas- vs. particle-phase fractions of a large number of SVOCs in real time in an urban area of East China with the use of a CHemical Analysis of aeRosols ONline (CHARON) inlet coupled to a high resolution Proton Transfer Reaction Time-of-Flight Mass Spectrometer (PTR-ToF-MS). We demonstrated the use of the CHARON inlet for highly efficient collection of particulate SVOCs while maintaining the intact molecular structures of these compounds. The collected month-long dataset with hourly resolution allows us to examine the gas-particle partitioning behaviors of a variety of SVOCs under different ambient conditions. By comparing the measurements with model predictions using the instantaneous equilibrium partitioning theory, we found that the dissociation of large parent molecules during the PTR ionization process likely introduces large uncertainties to the measured gas- vs. particle-phase fractions of less oxidized SVOCs, and therefore, caution should be taken when linking the molecular composition to the particle volatility when interpreting the PTR-ToF-MS data. Our analysis suggests that understanding the fragmentation mechanism of oxidized SVOCs and accounting for the neutral losses of small moieties during the molecular feature extraction from the raw mass spectra could reduce, to a large extent, the uncertainties associated with the gas-particle partitioning measurement of SVOCs in the ambient atmosphere.

1. Introduction

Gas-particle partitioning of semivolatile organic compounds (SVOCs) is a critical process involved in the formation and evolution of atmospheric organic aerosols (OA). Traditionally,

https://doi.org/10.5194/amt-2022-147
Preprint. Discussion started: 28 June 2022


Atmospheric Measurement Techniques Discussions

gas–particle equilibrium partitioning of organic substances is assumed to be established instantaneously (Zhang and Seinfeld, 2013), this assumption is in question if particles are semi-solid or glassy (Shiraiwa et al., 2013). Most studies to date addressing the kinetic limitations in partitioning have used indirect and/or theoretical methods that are lack of chemical and molecular specificity (Mai et al., 2015; Shiraiwa and Seinfeld, 2012). Direct measurements of gas-particle partitioning of SVOCs are needed in order to develop accurate parameterizations for the organic aerosol formation in climate models.

The major challenge in the characterization of gas-particle partitioning of SVOCs lies in the realtime measurement of labile compounds while maintaining their intact molecular structures with minimal fragmentation (Zhang et al., 2016a; Zhang et al., 2016b). In recent years, soft ionization techniques coupled to mass spectrometry have been widely used for the measurement of gas-phase SVOCs at the molecular level (Veres et al., 2008; Crounse et al., 2006; Heald and Kroll, 2020). Combined with thermal desorption methods, these techniques have also been deployed to measure organic compounds in both gas and particle phases nearly simultaneously (Krechmer et al., 2016). A notable example would be the use of the Filter Inlet for Gases and AEROsols coupled with the Chemical Ionization Mass Spectrometry (FIGAERO-CIMS) to quantify the gas-particle partitioning of a broad range of organic compounds in real time (Lopez-Hilfiker et al., 2014; Ye et al., 2021; Voliotis et al., 2021; Wang et al., 2020a; Lutz et al., 2019; Lee et al., 2018; Le Breton et al., 2018; Stark et al., 2017; Lopez-Hilfiker et al., 2016; Lopez-Hilfiker et al., 2015). A number of studies among those have reached a consensus that the thermograms method, i.e., using the calibrated thermal desorption profiles vs. temperature to derive the volatility, likely provides the best estimates of the actual phase distribution. In contrast, using the directly measured gas- and particle-phase fractions of

https://doi.org/10.5194/amt-2022-147
Preprint. Discussion started: 28 June 2022


Atmospheric Measurement Techniques Discussions

a given analyte will most likely introduce a significant positive or negative bias to the volatility estimation due to the thermal decomposition of labile organic compounds during the desorption process (Lopez-Hilfiker et al., 2015; Stark et al., 2017). Such thermal decomposition (or ion fragmentation) artifacts, either positive or negative depending on the molecular size, have been suggested to constitute the largest uncertainties in the estimation of phase partitioning behaviors of SVOCs using the thermal desorption method at ambient pressure (Thompson et al., 2016).

Along with the line of thermal desorption method development, an inlet designed for the CHemical Analysis of aeRosols ONline (CHARON) has been developed and coupled to the Proton Transfer Reaction Time-of-Flight Mass Spectrometer (PTR-ToF-MS) in recent years. As CHARON-PTR-ToF-MS does not rely on any form of pre-concentration on surfaces, it could provide online and direct measurements of organic compounds in both phases, compared with traditional thermal desorption instruments which still need to address artifacts during the particle collection and desorption processes. Another potential advantage of CHARON-PTR-ToF-MS is that the chemical information of the collected particles can be studied qualitatively and quantitatively over a chemical composition level even at sub-nanogram mass concentrations per molecule owing to the well studied ion-molecule reaction chemistry in PTR-ToF-MS (Piel et al., 2019). CHARON has shown promising potential in the realtime analysis of the chemical composition and spatiotemporal distributions of aerosols with laboratory-, ground-, and aircraft-based platforms (Piel et al., 2019; Tan et al., 2018; Gkatzelis et al., 2018a; Gkatzelis et al., 2018b; Muller et al., 2017; Eichler et al., 2017; Eichler et al., 2015; Antonsen et al., 2017; Leglise et al., 2019; Piel et al., 2021). As a relatively new technique, the use of CHARON-PTR-ToF-MS to investigate the gas-particle partitioning of organic compounds is still quite limited. Only one study by Gkatzelis et al. (2018b) deployed CHARON, together

https://doi.org/10.5194/amt-2022-147
Preprint. Discussion started: 28 June 2022


Atmospheric Measurement Techniques Discussions

with two other aerosol sampling inlets, to measure the OA formation and aging from monoterpenes and real plant emissions in chamber experiments. Whether the CHARON inlet can be applied to the study of gas-particle partitioning of organic compounds under the actual atmospheric conditions remains to be validated.

In this study, we assess the applicability of the CHARON inlet to the time-resolved collection of organic compounds in their native molecular state using laboratory tests with a series of authentic standards. We further employ the CHARON inlet coupled to a high resolution PTR-ToF-MS instrument to measure an array of gaseous and particulate SVOCs in an urban area of East China. The obtained month-long hourly dataset allows us to examine the gas-particle partitioning behaviors of SVOCs spanning a range of volatilities. By comparing the measurements with model predictions using the instantaneous equilibrium partitioning theory, we found that fragmentation during the PTR ionization process may introduce large uncertainties to the measured gas- vs. particle-phase fractions of less oxidized SVOCs. Understanding the dissociation patterns of parent molecules and accounting for the fragmentation losses when extracting the molecular features from the raw mass spectra are needed to improve the measured accuracy of SVOCs partitioning between the gas and particle phases.

2. Material and Methods

2.1. Sampling site

The sampling site located in the campus of the Shanghai Academy of Environmental Science (SAES) is representative of a typical urban environment with influences from heavy traffic, commercial, and residential activities (Liu et al., 2019). The sampling inlet of the PTR-ToF-MS instrument was installed on the roof of an eight-story building ~24 m above the ground.

https://doi.org/10.5194/amt-2022-147
Preprint. Discussion started: 28 June 2022


Atmospheric Measurement Techniques Discussions

A comprehensive measurement of gas- and particle-phase compounds in the ambient air was performed from Oct 24 to Nov 22. During the sampling period, the average temperature, relative humidity, and wind speed were 18.0 ± 3.0 °C, 61.0 ± 15.0%, and 1.8 ± 0.7 m/s, respectively.

2.2. CHARON-PTR-ToF-MS

2.2.1. Operation protocols

A Proton Transfer Reaction Time-of-Flight Mass Spectrometer (PTR-ToF-MS) coupled to a CHemical Analysis of aeRosols ONline (CHARON, Ionicon Analytik Inc, Innsbrunck, Austria) inlet was employed to measure the gas- and particle-phase concentrations of a series of SVOCs. The operating parameters of the PTR-ToF-MS were held constant during the entire measurement period. The drift tube pressure, temperature, and voltage were 2.9 mbar, 120 °C, and 500 V, respectively. These conditions correspond to an *E/N* (*E* is the electric field, and *N* is the number density of the gas molecules in the drift tube) value of ~100 Td (1 Td = 10^{-17} V cm^2) and a reaction time of 120 µs. Note that the *E/N* value determines the collision energy of ions in the reactor and therefore the degree of fragmentation and cluster formation. The operating conditions were selected for the purpose of relatively low fragmentation intensities (compared to 120–140 Td) and limited production of water clusters (compared to 60–80 Td). Low *E/N* enhances the degree of water clustering, which complicates the analysis of analyte ions due to a complex interplay between cluster formation ($RH^+(H_2O)_n$) and proton transfer reactions (Holzinger et al., 2019). During the campaign, the sensitivity of the PTR-ToF-MS was in the range of 300–1000 ncps ppb^{-1} and the mass resolution was maintained at ~5000 m/Δm. Mass spectra were collected at a time resolution of 10 s.

The CHARON inlet consists of 1) a gas-phase denuder (GPD) for stripping off gas-phase

https://doi.org/10.5194/amt-2022-147
Preprint. Discussion started: 28 June 2022


Atmospheric Measurement Techniques Discussions

analytes, 2) an aerodynamic lens (ADL) for particle collimation which is combined with an inertial sampler for emanating the particle-enriched flow, and 3) a thermo-desorption unit (TDU) for particle volatilization. The CHARON inlet functionality has been described in great detail by Eichler et al. (2015). The inlet we used here had a particle enrichment factor of ~15, as discussed shortly. The vaporizer (TDU) was operated at 140°C and ~8 mbar absolute pressure. Measurements of organic compounds in gas and particle phases were conducted using a parallel sampling system with two independent pumps, allowing for the selection of flow rates specifically adjusted for each phase, resulting in the overall residence time of less than 2 s (Fig. S1).

2.2.2. Sampling alternation between gas and particle phases

Gas-phase compounds were measured by directly sampling the ambient air via a 2 m long perfluoro-alkoxy (PFA) tube (1/4'' OD) capped with a polytetrafluoroethylene (PTFE) filter (Mitex^{TM} PTFE membrane, 5 µm pore size, 47 mm diameter) to prevent the clogging of particles in the PTR capillaries. The gas-phase inlet is independently connected to the PTR-ToF-MS instrument upstream of the drift tube via a pressure-controlled subsampling PEEK capillary (1/16'' OD). Zero measurements were performed by overflowing catalytically (platinum at 370°C) purified air through the inlet. Ambient particles were sampled through a stainless steel tube (3/8'' OD) with a flow rate of ~3 L min^{-1}, out of which a flow of ~500 ml min^{-1} was directed to the CHARON inlet. A $PM_{2.5}$ cyclone was installed in front of the sampling line to remove coarse particles (>2.5 µm). The particle-phase background was measured by placing a High-Efficiency Particulate Air filter (HEPA, HEPA-CAP 7, GE Healthcare UK Limited, Buckinghamshire, UK) upstream of the CHARON inlet. Servo motor activated valves made of passivated stainless steel were used for switching between the two inlet configurations.

https://doi.org/10.5194/amt-2022-147
Preprint. Discussion started: 28 June 2022


Atmospheric Measurement Techniques Discussions

During the campaign, CHARON-PTR-ToF-MS automatically switched between gas and particle phases every 15 min. Detailed setup is given in Fig. S1 in the Supporting Information.

The built-in PTR-manager software (Ionicon Analytik GmbH, Innsbruck, Austria) offers the possibility to program sequences by which the instrument switches between different settings. It takes ~ 1 min for gases and particles to re-equilibrate when switching between these two modes. Data generated during this transition period (~2 min) were not considered. Instrument background was measured for 15 min every 5h. The limits of detection (LoD) at 1 min resolution were in the range of 5.6 ± 2.9 ng m^{-3} for gases and 0.7 ± 0.5 ng m^{-3} for particles, respectively (Fig. S3). Concentrations of gaseous and particulate compounds shown here included the last 5 min of every gas/particle-phase working mode, in order to minimize the interferences carried over from the previous working mode by allowing for a sufficient amount of equilibration time in the inlet (Piel et al., 2021). In order to synchronize the gas- and particle-phase data to calculate gas-particle partitioning, the average hourly data were then used for further analysis.

2.2.3. Sensitivity and calibration

Weekly calibrations were performed using a multicomponent calibration gas standard (Linde, USA) at five concentration levels from 0.5 to 10 ppb (Fig. S2a). The calibration mixture includes methanol, acetonitrile, acetaldehyde, acrolein, acetone, isoprene, methyl vinyl ketone, methyl ethyl ketone, 2-pentanone, toluene, styrene, p-xylene, 1,3,5-trimethylbenzene, naphthalene and α-pinene. Here the sensitivity of PTR-ToF-MS is defined as the normalized ion intensity of RH^+ (ncps) obtained at a mixing ratio of 1 ppb. For a given species (R), its sensitivity (S, ncps ppb^{-1}) is a linear function of the rate constant of its reaction with H_3O^+ (k) :

https://doi.org/10.5194/amt-2022-147
Preprint. Discussion started: 28 June 2022

Atmospheric Measurement Techniques Discussions

$$S = \frac{\frac{I_{RH^+}}{I_{H_3O^+}} \times 10^6}{\frac{[R]}{N} \times 10^9} = k \times N \times 10^{-3} \times t \times \frac{T_{RH^+}}{T_{H_3O^+}} \times F_{RH^+} \quad (1)$$

$$\text{corrected } S = \frac{S}{\frac{T_{RH^+}}{T_{H_3O^+}} \times F_{RH^+}} = a \times k \quad (2)$$

The signals of H_3O^+ ($I_{H_3O^+}$) and RH^+ ions (I_{RH^+}) measured by the mass analyzer (in cps) can be related to the signals of H_3O^+ ($[H_3O^+]$) and RH^+ ($[RH^+]$) ions at the end of the drift tube, using their respective transmission efficiencies ($T_{H_3O^+}$ and T_{RH^+}) from the drift tube to the detector (De Gouw and Warneke, 2007). $[R]$ is the concentration of species R and N is the number density of gas in the drift tube. The reaction time (t) is determined by the ion drift velocity. F_{RH^+} represents the fraction of product ions detected as RH^+ ions ($0 \leq F_{RH^+} \leq 1$). For non-fragmenting compounds, $F_{RH^+} = 1$. The measured sensitivity is further corrected by accounting for fragmentation and transmission efficiency. The relative transmission efficiency of ions was derived from laboratory experiments (Fig. S2a). Fig. S2b shows a clear linear relationship between the corrected sensitivities of calibrated species and kinetic rate constants (k) for proton transfer reactions with H_3O^+. Following the method by Sekimoto et al. (2017), the linear regression result was used to determine the sensitivities of all uncalibrated species. The overall uncertainty was less than 15% for compounds with standards and around 50% for those without standards. Calculated sensitivity based on this method agrees well with measurements of authentic standards (Fig. S2c).

2.2.4. Enrichment factor

The CHARON inlet was calibrated routinely with pure ammonium nitrate particles to derive the enrichment factor as a function of the particle size following the procedures described in Eichler et al. (2015). In addition, we used a selection of authentic standards (Table S1) to test

https://doi.org/10.5194/amt-2022-147
Preprint. Discussion started: 28 June 2022


Atmospheric Measurement Techniques Discussions

the effect of desorption temperature on the enrichment factor of labile compounds. Previous studies with CHARON generally used a temperature of 140 °C to vaporize particles (Leglise et al., 2019; Gkatzelis et al., 2018b; Tan et al., 2018). Herein, we tested the TDU temperature ranging from 70 to 140°C. The selected chemical standards were individually dissolved in distilled water (ethanol in the case of 2-Pentadecanone and 1-Pentadecanol) and nebulized by an atomizer (TSI 3076, Shore-view, MN, USA) that was pressurized with ultrapure zero air. The nebulizer outflow was diverted through two diffusion dryers to remove water vapor and an activated charcoal denuder (NovaCarb F, Mast Carbon International Ltd., Guilford, UK) to remove organic vapors. The resulting flow of polydisperse particles was then delivered into a differential mobility analyzer (DMA, TSI 3080) for particle size selection. The transmitted particles at a given size bin (300 nm for organics and 100–450 nm range for ammonium nitrate) were introduced into the CHARON-PTR-ToF-MS analyzer and a condensation particle counter (CPC, TSI 3775), respectively. Particle mass concentrations were calculated based on the CPC number distribution measurements by assuming a shape factor of 0.8 for ammonium nitrate particles and 1 for organic particles, respectively.

The particle enrichment factor (*EF*) of a given analyte i was calculated as the ratio of the PTR-ToF-MS derived vs. CPC derived mass concentrations of analyte i at a given particle size bin:

$$VMR_{(\mathrm{PTR})\mathrm{i}} = \frac{I_\mathrm{i}}{S_\mathrm{i}} \quad (3)$$

$$VMR_{(\mathrm{CPC})\mathrm{i}} = \rho_\mathrm{i} \times V \times N_\mathrm{i} \times V_\mathrm{m} / Mw_\mathrm{i} \quad (4)$$

$$EF = \frac{VMR_{(\mathrm{PTR})\mathrm{i}}}{VMR_{(\mathrm{CPC})\mathrm{i}}} \quad (5)$$

Where I_i is the normalized signal of species i (ncps) by PTR-ToF-MS, S_i is the sensitivity

https://doi.org/10.5194/amt-2022-147
Preprint. Discussion started: 28 June 2022


Atmospheric Measurement Techniques Discussions

(ncps ppb^{-1}), VMR is the volume mixing ratio (ppb), ρ is the density of species i (g cm^{-3}), V is the volume of a particle sphere (m^3), N_i is the number concentration of particles measured by CPC (cm^{-3}), V_m is the molar volume of an ideal gas at 1 atm (22.4 L mol^{-1}), Mw_i is the molecular weight (g mol^{-1}). As the calculated sensitivities of most organics in the absence of authentic standards are subject to uncertainties (15%–50%), we will herein use the multiplication of EF and S_i to evaluate the combined effect of CHARON enrichment and sensitivity on the measured concentrations of a given analyte i in the particle phase.

2.2.5. Data processing

Data were analyzed using the Tofware package (v3.2.0, Tofwerk Inc), within the Igor Pro software (v7.0, Wavemetrics). Using this package, time-dependent mass calibrations were performed using four ions ($H_3{}^{18}O^+$, NO^+, $C_6H_5I^+$ and $C_6H_5I_2{}^+$), where $C_6H_5I^+$ and $C_6H_5I_2{}^+$ were produced from the internal standard di-iodobenzene. The relative mass deviation was within 6−8 ppm across the mass spectra. Considering the humidity dependence of reagent ions (H_3O^+ and $H_3O^+(H_2O)$), the fitted product ion signals (RH^+) were normalized to a standard reagent ion of 10^6 cps (counts per second). Elemental composition was determined based on the accurate m/z (mass to charge ratio) and isotopic pattern analysis. A list of ~1600 ions was extracted, including both gas- and particle-phase ions. Molecular formulas including only C, H, and O atoms were assigned to the detected ions by the addition of one proton in cases where the elemental composition analysis returned multiple options. About 85% of the signals were elementally resolved by the $C_xH_yO_z$ formula in ambient air mass spectra. A small number of nitrogen containing compounds, such as nitroaromatics, were also identified but not included in the following analysis. Throughout of the context, we use the word “species” to refer to all compounds with assigned molecular formula, which may include multiple isomers.

https://doi.org/10.5194/amt-2022-147
Preprint. Discussion started: 28 June 2022

Atmospheric Measurement Techniques Discussions

2.3. Complementary measurements

In addition to CHARON-PTR-ToF-MS, a Thermal desorption Aerosol Gas chromatograph (TAG) was also employed to measure a series of particle-phase organic species. Details of the TAG operation and data analysis protocols can be found in previous studies (He et al., 2020; Wang et al., 2020b; Zhu et al., 2021). The elemental composition and mass concentration of particles were measured by an Aerodyne high-resolution time-of-flight Aerosol Mass Spectrometer (AMS), with details of operation and quality control protocols given by our recent study (Huang et al., 2021). Volatile organic compounds (VOC, C_2–C_{12}) were analyzed by a custom-built online gas chromatography system equipped with a mass spectrometer and a flame ionization detector (GC-MS/FID). The performance of this system can be found in our previous publications (Zhu et al., 2018; Wang et al., 2014). Meteorological parameters (ambient temperature, wind speed, wind direction, and relative humidity) were collected by an automatic weather station (Metone 590 series) mounted on the roof top of the campaign site.

2.4. Gas-particle partitioning measurements vs. modeling

The CHARON-PTR-ToF-MS measured gas- and particle-phase concentrations of a given species i can be used to calculate its particle-phase fraction ($F_{p,i}$).

$$P_i = \frac{\frac{I_{p,i} \times \left(\frac{m}{z_i} - 1\right)}{V_m \times S_i}}{EF} \quad (6)$$

$$G_i = \frac{I_{g,i} \times \left(\frac{m}{z_i} - 1\right)}{V_m \times S_i} \quad (7)$$

$$F_{p,i} = \frac{P_i}{P_i + G_i} \quad (8)$$

Where P_i and G_i are the mass concentrations (ng m^{-3}) of species i in the particle and gas phases, respectively. $I_{p,i}$ and $I_{g,i}$ are the normalized signal (ncps) of the PTR-ToF-MS

https://doi.org/10.5194/amt-2022-147
Preprint. Discussion started: 28 June 2022


Atmospheric Measurement Techniques Discussions

detected ion i in the particle and gas phases, respectively. V_m is taken as 22.4 L/mol. S_i is calculated or measured sensitivity (ncps ppb^{-1}), see details in Section 2.2.3. As structural isomers cannot be resolved in the mass spectra, the calculation here assumes that all isomers with the same molecular formula have the same chemical properties, i.e., saturation vapor pressures.

Gas-particle partitioning of a given analyte i was also modeled using the equilibrium partitioning theory (Pankow, 1994):

$$F_{p,i} = \frac{1}{1 + C_i^* / C_{OA}} \quad (9)$$

$$C_i^* = \frac{10^6 Mw_i \zeta_i p_i}{RT} \quad (10)$$

Where C_{OA} is the organic aerosol concentration measured by AMS (μg m^{-3}), C_i^* is the saturation mass concentration (μg m^{-3}), Mw_i is the molecular weight (g mol^{-1}), ζ is the activity coefficient (assumed as unity), p_i is the pure component liquid vapor pressure (Pa), R is the universal gas constant (8.2 × 10^{-5} m^3 atm K^{-1} mol^{-1}), and T is the ambient temperature (K). As detailed chemical information is lacking for all species detected by PTR-ToF-MS, here we use the expression given by Donahue et al. (2011) to approximate the value of C_i^*:

$$\log_{10} C_i^* = \left(n_C^0 - n_C^i\right) b_C - n_O^i b_O - 2 \frac{n_C^i n_O^i}{n_C^i + n_O^i} b_{CO} \quad (11)$$

Where $n_C^0 = 25$, $b_C = 0.475$, $b_O = 2.3$, and $b_{CO} = -0.3$

3. Results and Discussion

3.1. Particle enrichment: effect of desorption temperature

Thermal desorption as a common procedure used in the chemical characterization of organic aerosols is often susceptible to fragmentation of non-refractory compounds. Due to the

https://doi.org/10.5194/amt-2022-147
Preprint. Discussion started: 28 June 2022


Atmospheric Measurement Techniques Discussions

high temperature used to evaporate particles collected, labile and large molecules are inevitably subject to fragmentation, thereby introducing large uncertainties to the measured mass and composition of the particulate organic compounds (Lopez-Hilfiker et al., 2015; Yatavelli et al., 2012; Zhao et al., 2013). Thermal decomposition of oxidized organic compounds has been observed at vaporizer temperature as low as 200 °C, the lowest temperature required to vaporize OA as reported (Stark et al., 2017). While decreasing the vaporizer temperature is necessary to maintain the intact structure of labile molecules, low temperature (e.g., 85 °C) however fails to completely evaporate the collected particles into vapors, resulting in an underestimation of the collected OA mass (Inomata et al., 2014). Here we performed a series of sensitivity tests to identify the optimal vaporizer temperature in the CHARON inlet for the measurements of organic compounds in the particle phase.

Prior to the temperature sensitivity test, we have validated that the particle enrichment factor, also known as collection efficiency and defined as the ratio of the particle mass concentration upstream to downstream of the aerodynamic lens, does not depend on the particle size. As shown in Fig. 1a, the measured *EF* value for ammonium nitrate particles, detected as NO_2^+ produced from the nitric acid vapor, remains constant as ~15 in the 150–450 nm particle size range. The lower values in the 100–150 nm size range can be explained by the lower particle transmission efficiency in the gas phase denuder, e.g., 75%–80% for 100 nm particles (Eichler et al., 2015). Also, particles below 150 nm are less efficiently concentrated in the subsampling flow after the aerodynamic lens. Therefore, we used the monodisperse particles generated from selected organic standards at 300 nm for the temperature sensitivity test.

A number of chemical standards that are representative of alcohols, carbonyls, and carboxylic acids and with the vapor pressure ranging from 10^{-14} to 10^{-1} Pa (at 25 °C, taken from

https://doi.org/10.5194/amt-2022-147
Preprint. Discussion started: 28 June 2022


Atmospheric Measurement Techniques Discussions

EPA EPI Suite (2012), see values given in Table S1) were used to generate organic aerosols, which, upon size selection at 300 nm, were directed to the CHARON inlet. Particle evaporation occurs downstream of the aerodynamic lens in the gas phase and on the tube and orifice surface to which submicron particles rapidly diffuse at ~8 mbar operating pressure. The thermal desorption unit was designed to ensure that ammonium sulfate particles (10^{-20} Pa) can be completely evaporated (Piel et al., 2019; Eichler et al., 2015). As the desorption temperature was varied from 70 °C to 140 °C, the intensities of all detected ions (including both parent and fragment ions) for each organic standard analyzed were stable within 15%, as shown in Fig. 1b. Also note that we did not observe any ions produced from decarboxylation and/or dehydration during the particle evaporation process. This is because the relative low operation temperature and the short heat exposure time could effectively limit any thermal dissociation of organic molecules. This demonstrates that the parent molecule fragmentation, if any, does not occur under the range of desorption temperature used in the CHARON inlet, but rather results from the ionic dissociation process in the ionization chamber of the PTR-ToF-MS instrument. We therefore used the sum total of intensities of all major ions detected as the PTR-ToF-MS response to a given organic standard analyzed. Fig. 1c shows that the derived enrichment factors stay constant for all compounds investigated (Mw ~ 160–230 g/mol). The relative signals of all fragment ions are stable over the range of the desorption temperature as shown in Fig. 2. This suggests that the desorption temperature used here, even as low as 70 °C, is sufficient to evaporate SVOCs (volatility > 10^{-14} Pa at 25 °C), due to the low operating pressure (~8 mbar) that significantly enhances the partitioning shift to the gas phase. One low volatility compound, sucrose (Mw is 342 g/mol and vapor pressure is 4.69×10^{-14} Pa), has a slightly lower enhancement factor compared with all the other organic standards tested. This is mainly due to

https://doi.org/10.5194/amt-2022-147
Preprint. Discussion started: 28 June 2022

Atmospheric Measurement Techniques Discussions

333 the intensive dehydration of the parent compound in the ionization chamber and as a result,
334 only a few fragment ions were captured, resulting in a lower PTR response and thereby lower
335 *EF* value calculated from Equations (3-5).

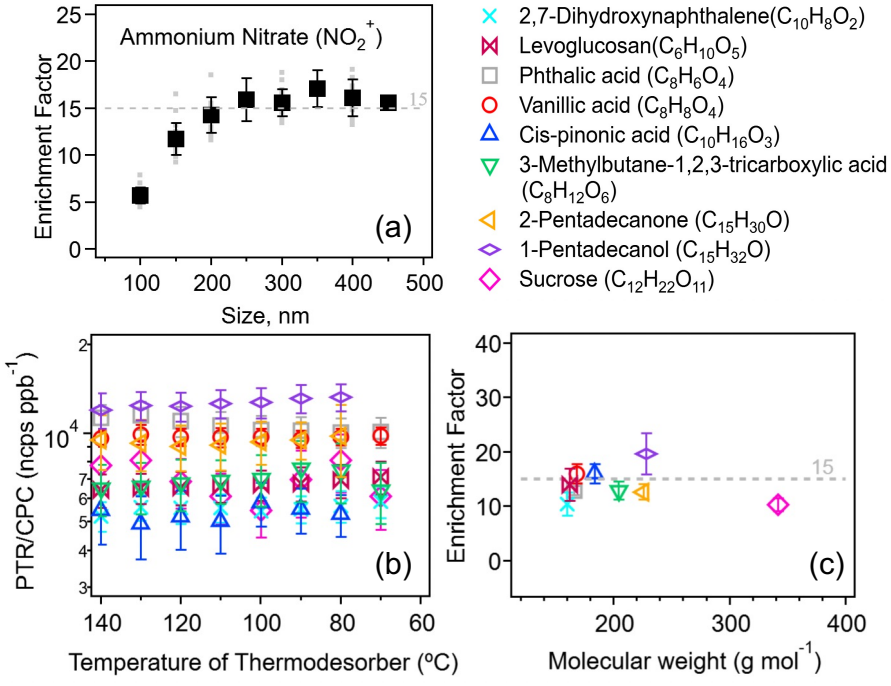

336

337 Figure 1. (a) Measured unitless enrichment factor (*EF*) of ammonium nitrate particles as a
338 function of particle size in the 100–450 nm range. Grey markers represent all replicating
339 measurements. The error bar denotes one standard deviation (1σ) of the average. (b) Ratios of
340 PTR-ToF-MS signals to CPC counts (±1σ) for all organic standards studied. (c) *EF* (±1σ) of
341 different compounds based on the calculated sensitivity.

342

https://doi.org/10.5194/amt-2022-147
Preprint. Discussion started: 28 June 2022

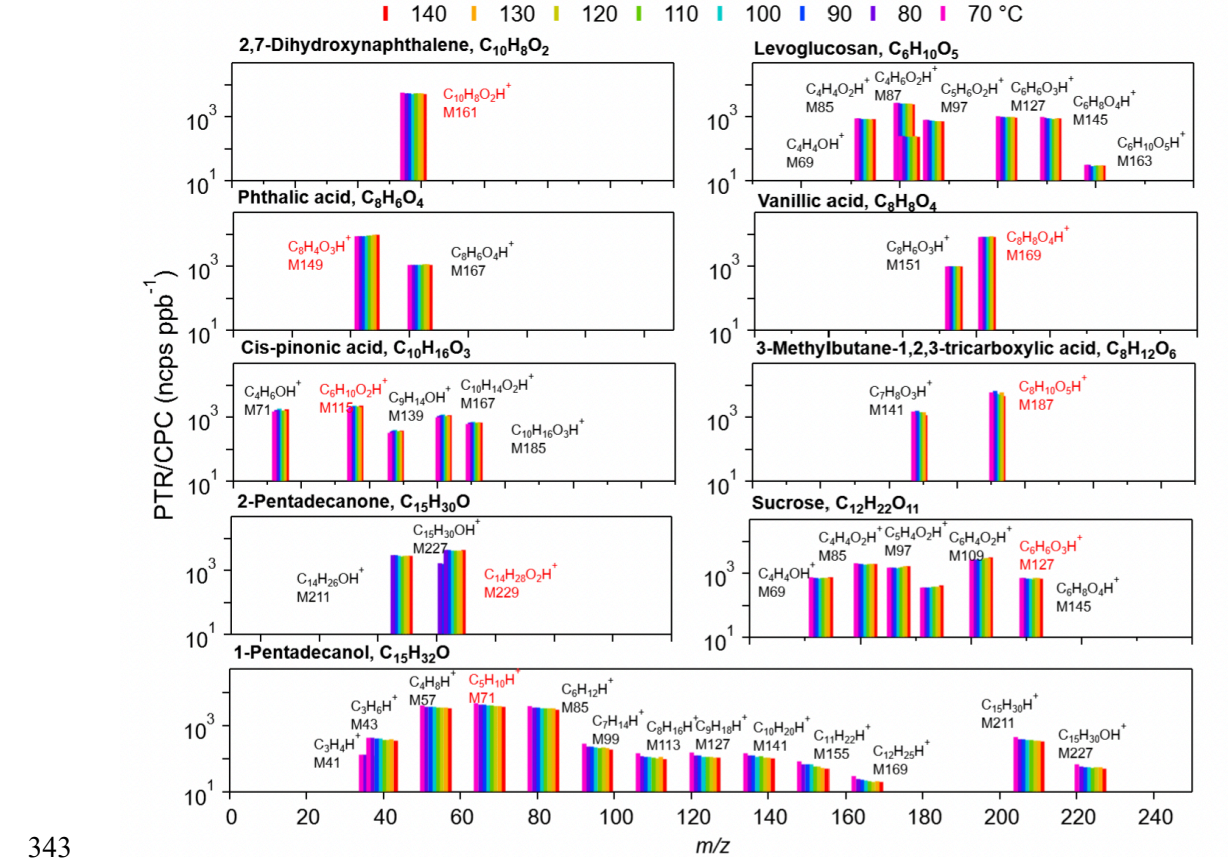

Figure 2. PTR-ToF-MS signals (ncps) normalized to the corresponding CPC measurements (ppb) of all detected ions (including both parent and fragments) for a given pure organic standard tested under different desorption temperatures (70–140 °C).

3.2. Molecular features of detected organic species

A comparison of PTR-ToF-MS measurements with other techniques available on site was performed for both gas and particle phases. For the gas phase, quantitative measurements of VOCs by GC-MS/FID, including ketones and aromatics, agree very well with corresponding PTR-ToF-MS measurements, as shown in Fig. S4. For the particle phase, the time series of a

https://doi.org/10.5194/amt-2022-147
Preprint. Discussion started: 28 June 2022

Atmospheric Measurement Techniques Discussions

353 group of $C_xH_yO_4$ species (including $C_4H_6O_4$, $C_5H_8O_4$, $C_6H_{10}O_4$, and $C_8H_6O_4$) correlate well with
354 corresponding measurements taken by TAG (r ~ 0.60–0.80). But the CHARON-PTR-ToF-MS
355 measured total carbon mass is generally lower than the TAG measurements by a factor of 2 to
356 6 (Fig. S5). This is likely caused by the fragmentation (e.g., loss of H_2O, see Fig. S6) of the
357 parent compounds during the ionization process, as discussed in detail in Section 3.3. The time
358 series of total OA mass detected by CHARON-PTR-ToF-MS also agree with the AMS
359 measurements (r ~ 0.91). Previous studies have reported those particulate organics measured
360 by PTR-MS with a thermal desorption inlect account for 25%–60% carbon mass of the total
361 organic aerosols measured by AMS (Holzinger et al., 2013). Direct comparison of the total OA
362 mass loading is not applicable here since the CHARON-PTR-ToF-MS measurements only
363 focused on compounds with the mass to charge ratio below 250 Th.

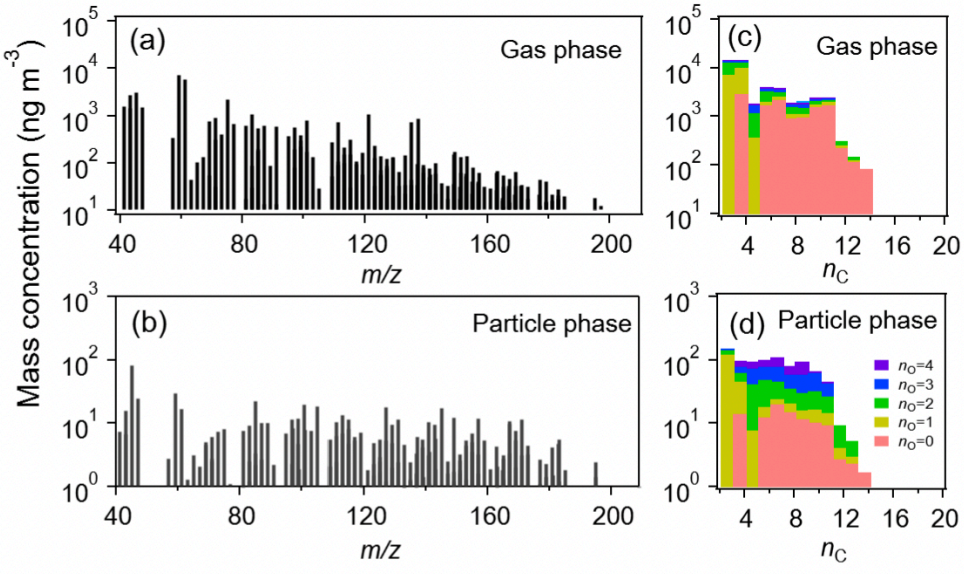

364

365 Figure 3. Monthly-averaged PTR-ToF-MS mass spectra (background subtracted) in the (a) gas
366 phase and (b) particle phase. Mass distributions of all identified species resolved by the carbon

https://doi.org/10.5194/amt-2022-147
Preprint. Discussion started: 28 June 2022


Atmospheric Measurement Techniques Discussions

and oxygen numbers (n_C and n_O) in the (c) gas phase and (d) particle phase.

Fig. 3 (a-b) shows the PTR-ToF-MS spectra of dominant ions averaged over the entire campaign in both gas and particle phases. The mass concentrations of individual ions are in the range of 7.9–7179.3 ng m^{-3} in the gas phase and 0.6–82.7 ng m^{-3} in the particle phase. A total of 152 species (with >60% data points above the PTR-ToF-MS detection limit) are identified, contributing to ~69% and ~44%, respectively, of the total organic mass measured in the gas and particle phases. The molecular distribution characterized by the carbon and oxygen of these species is given in Fig. 3 (c-d). The most abundant species are characterized by a generic formula of C_xH_yO and $C_xH_yO_2$, resolving ~64% and ~46% in total of all identified species in the gas and particle phases, respectively. Another dominant component in the gas phase is hydrocarbon-like compounds (C_xH_y) (~27%), which contribute ~12% of the organic mass in the particle phase. Species with higher oxygen numbers (>2) contribute to a large fraction (~42%) of the total particulate mass. These $C_xH_yO_{1\text{-}4}$ groups exhibit different diurnal cycles, as shown in Fig. S7, reflecting their unique formation chemistry. The C_xH_y group peaks in the early morning rush hour and likely originates from primary traffic emissions. On the contrary, both $C_xH_yO_3$ and $C_xH_yO_4$ groups peak at noon, suggesting a strong secondary formation source. The diurnal trends for C_xH_yO and $C_xH_yO_2$ groups are relatively flat during the day, likely indicative of an intertwined primary emission and secondary formation processes.

3.3. Measured vs. modeled gas-particle partitioning

Fig. 4 shows the calculated particle-phase fraction (F_p) of the identified 152 species using the CHARON-PTR-ToF-MS measurements in both phases. It is important to note that an

https://doi.org/10.5194/amt-2022-147
Preprint. Discussion started: 28 June 2022


Atmospheric Measurement Techniques Discussions

authentic standard is not required for the calculation of F_p for any given species, because the PTR sensitivity term is essentially canceled in the divisor function in Equations (6-8). Also given in Fig. 4 is the simulated F_p of the derived molecular formulas of all species identified using the equilibrium partitioning theory, see method described in Section 2.4. Interestingly, for oxidized species i.e., $C_xH_yO_4$, the measured F_p agrees with the simulations, as shown in Fig. 4a. As the oxygen number decreases, the measured F_p values tend to deviate from the simulations by up to several orders of magnitude (e.g., C_xH_y). Note that these less oxidized compounds are mostly small molecules and they are highly unlikely present in the condensed phase as closed-shell monomers (Pankow and Asher, 2008; Holzinger et al., 2010). Rather, they are most likely fragments produced from the decomposition of large molecules, which no surprisingly would favor partitioning in the particle phase. The discrepancy in the measurement-model comparison underscores the importance of understanding the fragmentation mechanism during ionization when extracting molecular features from the raw PTR mass spectra.

Parent-ion fragmentation in PTR-MS instruments has been widely observed (Pagonis et al., 2019). Oxygenates exhibit trends in neutral losses of water or saturated alcohols. Here, we apply a correction to the molecular formula of the 152 identified species by assuming that these species are fragments produced from their parent precursors through the neutral loss of a carboxyl group ($-CO_2$), a carbonyl group (-CO), a hydroxyl group ($-H_2O$), or an alcohol group ($-C_2H_6O$). By applying this correction, the modeled F_p of a given species $C_xH_yO_z$ would actually represent the particle-phase fraction of the its parent species $C_xH_yO_z{\bullet}CO_2$, $C_xH_yO_z{\bullet}CO$, $C_xH_yO_z{\bullet}H_2O$, or $C_xH_yO_z{\bullet}C_2H_6O$,. As shown in Fig. 4 (b-e), such a correction could significantly increase the modeled F_p values by several orders of magnitude. The assumption of neutral

https://doi.org/10.5194/amt-2022-147
Preprint. Discussion started: 28 June 2022


Atmospheric Measurement Techniques Discussions

losses of CO_2 or C_2H_6O allows for much improved agreement between modeled vs. measured F_p values for less oxidized species. This implies that these small and less oxidized species are likely fragments resulting from the decomposition of large parent precursors. As our particle enrichment test (details given in Section 3.1) has confirmed that the thermal desorption temperature employed for particle evaporation does not lead to any intensive fragmentation, thus the collision-induced dissociation during the proton transfer reaction process becomes the predominant process that produces fragments (Lindinger et al., 1998; Gueneron et al., 2015; Gkatzelis et al., 2018b). Although the electric field applied to the drift tube is considered low to moderate compared with most previous PTR-MS measurements (E/N ~ 100 Td in this study vs. E/N ~ 140 Td commonly found in PTR-MS measurements) (Yuan et al., 2017), parent-ion fragmentation was still widely observed here and complicated the mass spectra interpretation and molecular feature extraction. While some recent CHARON measurements employed lower electric field in the drift tube (E/N ~ 60 Td) (Leglise et al., 2019; Gkatzelis et al., 2018a; Piel et al., 2019), such conditions could promote the formation of water cluster ions, which increase with humidity and reduce the PTR sensitivity, and therefore are not ideally suitable for our field measurements. A compromise solution would be using a moderate electric field in the drift tube (e.g., ~ 100 Td) and meanwhile applying appropriate molecular corrections to all ions detected in the mass spectra by considering possible neutral losses of small moieties as practiced in Fig. 4.

https://doi.org/10.5194/amt-2022-147
Preprint. Discussion started: 28 June 2022

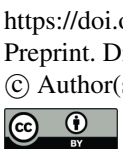

Atmospheric Measurement Techniques Discussions

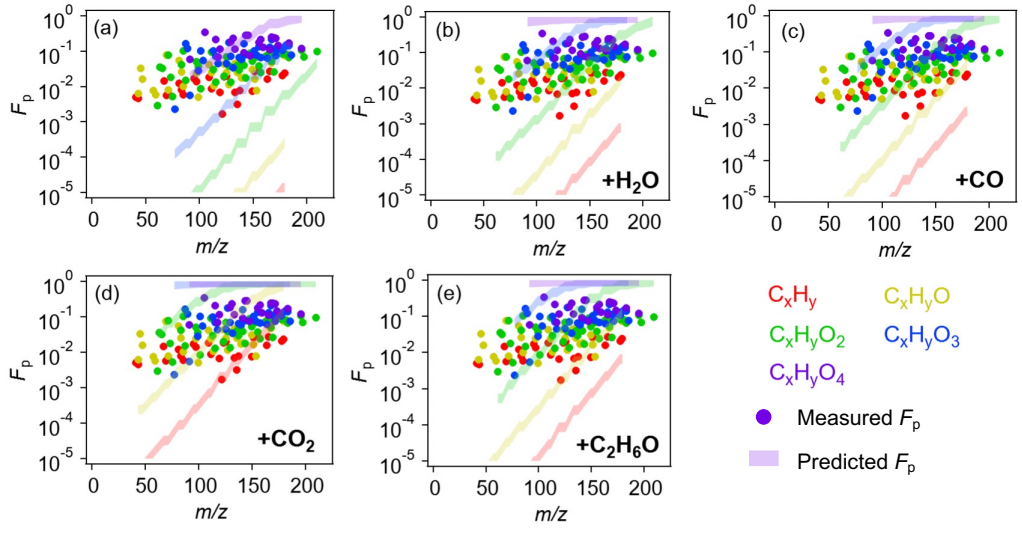

Figure 4. (a) Campaign average fraction (F_p) of organic species in the particle-phase grouped by the oxygen number. Solid markers represent the calculated F_p based on the CHARON-PTR-ToF-MS measurements. Colored shades represent the predicted F_p of corresponding molecular formulas. (b-e) Measured vs. predicted F_p assuming the identified species are fragments of corresponding parent compounds through neutral losses of H_2O, CO, CO_2, and C_2H_6O.

4. Conclusions

Recent studies have suggested that some of the model-measurement discrepancies in the representation of ambient organic aerosol budget might be due to the nonequilibrium gas/particle partitioning caused by kinetic limitations in the presence of glassy or semi-solid phase (Perraud et al., 2012; Mai et al., 2015; Shiraiwa et al., 2013). It is therefore necessary to validate whether the equilibrium partitioning theory could adequately describe the condensation of semivolatile organic vapors onto atmospheric aerosols under ambient conditions, and the accurate measurement of these SVOCs in both gas and particle phases is

https://doi.org/10.5194/amt-2022-147
Preprint. Discussion started: 28 June 2022


Atmospheric Measurement Techniques Discussions

the crucial prerequisite. In this study, we have employed the PTR-ToF-MS instrument coupled to a CHARON inlet, together with a suite of complementary measurements, to characterize the atmospheric partitioning behaviors of an array of SVOCs at an urban site of East China. Prior to the application to the field measurements, we first performed a series of laboratory experiments to test whether the CHARON inlet is capable of sampling organic molecules (including alcohols, carbonyls, and carboxylic acids) in their native states and structures. With the low pressure condition used in the CHARON inlet, a thermal desorption temperature less than 140 °C could adequately evaporate organic compounds with vapor pressure higher than 10^{-14} Pa while minimizing the thermal decomposition of labile functionalities. The auto-switch function between the gas and particle mode with one single PTR-ToF-MS instrument could monitor gaseous and particulate organic compounds in real time, thereby providing important information of their partitioning behaviors in the ambient atmosphere. Particle-phase fractions of a total of 152 organic species were derived from the CHARON-PTR-ToF-MS measurements and further compared with model predictions using the instantaneous equilibrium partitioning theory. While the model captured the particle-phase fraction of oxidized compounds (e.g., $C_xH_yO_{3\text{-}4}$), predictions of less oxidized compounds, notably the C_xH_y family, differ from the corresponding measurements by several orders of magnitude. Such a large discrepancy is very likely caused by the intensive fragmentation of the parent organic compounds during the ionization process in PTR-ToF-MS. Accounting for common fragmentation patterns in the simulations of gas-particle partitioning, i.e., neutral losses of $-CO_2$, $-CO$, $-H_2O$, or $-C_2H_6O$, could significantly improve the model-measurement agreement. Such corrections are very necessary towards an accurate measurement of both particle- and gas-phase SVOCs using the CHARON-PTR-ToF-MS. Our study suggests the crucial importance of optimizing operation

https://doi.org/10.5194/amt-2022-147
Preprint. Discussion started: 28 June 2022


Atmospheric Measurement Techniques Discussions

conditions and understanding the fragmentation mechanism in the particle collection, vaporization, and ionization processes in understanding the gas-particle partitioning behaviors of organic compounds using any thermal desorption based aerosol measurement method.

Data availability. The data shown in the paper are available upon request from the corresponding author.

Author Contributions. YP carried out experiments and measurements and drafted the manuscript. HW and XZ designed the experimental studies, supervised the laboratory work and wrote the manuscript. YG and SJ supported the ambient measurements. SZ, DH, PH, and SL supported the data analysis. TC and CH supervised the scientific work. All authors have given approval to the final version of the manuscript.

Competing interests. The authors declare no competing financial interest.

Acknowledgements. This research has been supported by the National Natural Science Foundation of China (No. 42175135, No. 42175179) and the Shanghai Science and Technology Commission of the Shanghai Municipality (No. 20ZR1447800).

References

Antonsen, S., Bunkan, A. J. C., D'Anna, B., Eichler, P., Farren, N., Hallquist, M., Hamilton, J. F., Kvarnliden, H., Mikoviny, T., Muller, M., Nielsen, C. J., Stenstrom, Y., Tan, W., Wisthaler, A., and Zhu, L.: Atmospheric chemistry of tert-butylamine and AMP, in: Enrgy Proced, edited by: Dixon, T., Laloui, L., and Twinning, S., Energy Procedia, Elsevier Science Bv, Amsterdam, 1026-1032, 10.1016/j.egypro.2017.03.1248, 2017.

https://doi.org/10.5194/amt-2022-147
Preprint. Discussion started: 28 June 2022


Atmospheric Measurement Techniques Discussions

493 Crounse, J. D., McKinney, K. A., Kwan, A. J., and Wennberg, P. O.: Measurement of gas-phase
494 hydroperoxides by chemical ionization mass spectrometry, Anal. Chem., 78, 6726-6732,
495 10.1021/ac0604235, 2006.

496 de Gouw, J. and Warneke, C.: Measurements of volatile organic compounds in the earths
497 atmosphere using proton-transfer-reaction mass spectrometry, Mass Spectrometry Reviews, 26,
498 223-257, 10.1002/mas.20119, 2007.

499 Donahue, N. M., Epstein, S. A., Pandis, S. N., and Robinson, A. L.: A two-dimensional
500 volatility basis set: 1. organic-aerosol mixing thermodynamics, Atmos. Chem. Phys., 11, 3303-
501 3318, 10.5194/acp-11-3303-2011, 2011.

502 Eichler, P., Muller, M., D'Anna, B., and Wisthaler, A.: A novel inlet system for online chemical
503 analysis of semi-volatile submicron particulate matter, Atmos. Meas. Tech., 8, 1353-1360,
504 10.5194/amt-8-1353-2015, 2015.

505 Eichler, P., Muller, M., Rohmann, C., Stengel, B., Orasche, J., Zimmermann, R., and Wisthaler,
506 A.: Lubricating Oil as a Major Constituent of Ship Exhaust Particles, Environ. Sci. Technol.
507 Lett., 4, 54-58, 10.1021/acs.estlett.6b00488, 2017.

508 EPA: Estimation Program Interface (EPI) Suite (v4.11), US [code], 2012.

509 Gkatzelis, G. I., Tillmann, R., Hohaus, T., Muller, M., Eichler, P., Xu, K. M., Schlag, P., Schmitt,
510 S. H., Wegener, R., Kaminski, M., Holzinger, R., Wisthaler, A., and Kiendler-Scharr, A.:
511 Comparison of three aerosol chemical characterization techniques utilizing PTR-ToF-MS: a
512 study on freshly formed and aged biogenic SOA, Atmos. Meas. Tech., 11, 1481-1500, 2018a.

https://doi.org/10.5194/amt-2022-147
Preprint. Discussion started: 28 June 2022


Atmospheric Measurement Techniques Discussions

513 Gkatzelis, G. I., Hohaus, T., Tillmann, R., Gensch, I., Muller, M., Eichler, P., Xu, K. M., Schlag,
514 P., Schmitt, S. H., Yu, Z. J., Wegener, R., Kaminski, M., Holzinger, R., Wisthaler, A., and
515 Kiendler-Scharr, A.: Gas-to-particle partitioning of major biogenic oxidation products: a study
516 on freshly formed and aged biogenic SOA, Atmos. Chem. Phys., 18, 12969-12989,
517 10.5194/acp-18-12969-2018, 2018b.

518 Gueneron, M., Erickson, M. H., VanderSchelden, G. S., and Jobson, B. T.: PTR-MS
519 fragmentation patterns of gasoline hydrocarbons, International Journal of Mass Spectrometry,
520 379, 97-109, 10.1016/j.ijms.2015.01.001, 2015.

521 He, X., Wang, Q., Huang, X. H. H., Huang, D. D., Zhou, M., Qiao, L., Zhu, S., Ma, Y.-g., Wang,
522 H.-l., Li, L., Huang, C., Xu, W., Worsnop, D. R., Goldstein, A. H., and Yu, J. Z.: Hourly
523 measurements of organic molecular markers in urban Shanghai, China: Observation of
524 enhanced formation of secondary organic aerosol during particulate matter episodic periods,
525 Atmos. Environ., 240, 10.1016/j.atmosenv.2020.117807, 2020.

526 Heald, C. L. and Kroll, J. H.: The fuel of atmospheric chemistry: Toward a complete description
527 of reactive organic carbon, Sci. Adv., 6, 10.1126/sciadv.aay8967, 2020.

528 Holzinger, R., Goldstein, A. H., Hayes, P. L., Jimenez, J. L., and Timkovsky, J.: Chemical
529 evolution of organic aerosol in Los Angeles during the CalNex 2010 study, Atmos. Chem. Phys.,
530 13, 10125-10141, 10.5194/acp-13-10125-2013, 2013.

531 Holzinger, R., Williams, J., Herrmann, F., Lelieveld, J., Donahue, N. M., and Rockmann, T.:
532 Aerosol analysis using a Thermal-Desorption Proton-Transfer-Reaction Mass Spectrometer
533 (TD-PTR-MS): a new approach to study processing of organic aerosols, Atmos. Chem. Phys.,

https://doi.org/10.5194/amt-2022-147
Preprint. Discussion started: 28 June 2022

534 10, 2257-2267, 10.5194/acp-10-2257-2010, 2010.

535 Holzinger, R., Acton, W. J. F., Bloss, W. J., Breitenlechner, M., Crilley, L. R., Dusanter, S.,
536 Gonin, M., Gros, V., Keutsch, F. N., Kiendler-Scharr, A., Kramer, L. J., Krechmer, J. E.,
537 Languille, B., Locoge, N., Lopez-Hilfiker, F., Materić, D., Moreno, S., Nemitz, E., Quéléver,
538 L. L. J., Sarda Esteve, R., Sauvage, S., Schallhart, S., Sommariva, R., Tillmann, R., Wedel, S.,
539 Worton, D. R., Xu, K., and Zaytsev, A.: Validity and limitations of simple reaction kinetics to
540 calculate concentrations of organic compounds from ion counts in PTR-MS, Atmos. Meas.
541 Tech., 12, 6193-6208, 10.5194/amt-12-6193-2019, 2019.

542 Huang, D. D., Zhu, S., An, J., Wang, Q., Qiao, L., Zhou, M., He, X., Ma, Y., Sun, Y., Huang,
543 C., Yu, J. Z., and Zhang, Q.: Comparative Assessment of Cooking Emission Contributions to
544 Urban Organic Aerosol Using Online Molecular Tracers and Aerosol Mass Spectrometry
545 Measurements, Environ. Sci. Technol., 10.1021/acs.est.1c03280, 2021.

546 Inomata, S., Sato, K., Hirokawa, J., Sakamoto, Y., Tanimoto, H., Okumura, M., Tohno, S., and
547 Imamura, T.: Analysis of secondary organic aerosols from ozonolysis of isoprene by proton
548 transfer reaction mass spectrometry, Atmos. Environ., 97, 397-405,
549 10.1016/j.atmosenv.2014.03.045, 2014.

550 Krechmer, J. E., Groessl, M., Zhang, X., Junninen, H., Massoli, P., Lambe, A. T., Kimmel, J.
551 R., Cubison, M. J., Graf, S., Lin, Y.-H., Budisulistiorini, S. H., Zhang, H., Surratt, J. D.,
552 Knochenmuss, R., Jayne, J. T., Worsnop, D. R., Jimenez, J.-L., and Canagaratna, M. R.: Ion
553 mobility spectrometry–mass spectrometry (IMS–MS) for on- and offline analysis of
554 atmospheric gas and aerosol species, Atmos. Meas. Tech., 9, 3245-3262, 10.5194/amt-9-3245-

https://doi.org/10.5194/amt-2022-147
Preprint. Discussion started: 28 June 2022


Atmospheric Measurement Techniques Discussions

555 2016, 2016.

556 Le Breton, M., Wang, Y. J., Hallquist, A. M., Pathak, R. K., Zheng, J., Yang, Y. D., Shang, D.
557 J., Glasius, M., Bannan, T. J., Liu, Q. Y., Chan, C. K., Percival, C. J., Zhu, W. F., Lou, S. R.,
558 Topping, D., Wang, Y. C., Yu, J. Z., Lu, K. D., Guo, S., Hu, M., and Hallquist, M.: Online gas-
559 and particle-phase measurements of organosulfates, organosulfonates and nitrooxy
560 organosulfates in Beijing utilizing a FIGAERO ToF-CIMS, Atmos. Chem. Phys., 18, 10355-
561 10371, 2018.

562 Lee, B. H., Lopez-Hilfiker, F. D., D'Ambro, E. L., Zhou, P., Boy, M., Petäjä, T., Hao, L.,
563 Virtanen, A., and Thornton, J. A.: Semi-volatile and highly oxygenated gaseous and particulate
564 organic compounds observed above a boreal forest canopy, Atmos. Chem. Phys., 18, 11547-
565 11562, 10.5194/acp-18-11547-2018, 2018.

566 Leglise, J., Muller, M., Piel, F., Otto, T., and Wisthaler, A.: Bulk Organic Aerosol Analysis by
567 Proton-Transfer-Reaction Mass Spectrometry: An Improved Methodology for the
568 Determination of Total Organic Mass, O:C and H:C Elemental Ratios, and the Average
569 Molecular Formula, Anal. Chem., 91, 12619-12624, 10.1021/acs.analchem.9b02949, 2019.

570 Lindinger, W., Hansel, A., and Jordan, A.: Proton-transfer-reaction mass spectrometry (PTR-
571 MS): on-line monitoring of volatile organic compounds at pptv levels, Chem. Soc. Rev., 27,
572 347-354, 10.1039/a827347z, 1998.

573 Liu, Y., Wang, H., Jing, S., Gao, Y., Peng, Y., Lou, S., Cheng, T., Tao, S., Li, L., Li, Y., Huang,
574 D., Wang, Q., and An, J.: Characteristics and sources of volatile organic compounds (VOCs) in
575 Shanghai during summer: Implications of regional transport, Atmos. Environ., 215,

https://doi.org/10.5194/amt-2022-147
Preprint. Discussion started: 28 June 2022


Atmospheric Measurement Techniques Discussions

576 10.1016/j.atmosenv.2019.116902, 2019.

577 Lopez-Hilfiker, F. D., Mohr, C., Ehn, M., Rubach, F., Kleist, E., Wildt, J., Mentel, T. F., Lutz,
578 A., Hallquist, M., Worsnop, D., and Thornton, J. A.: A novel method for online analysis of gas
579 and particle composition: description and evaluation of a Filter Inlet for Gases and AEROsols
580 (FIGAERO), Atmos. Meas. Tech., 7, 983-1001, 10.5194/amt-7-983-2014, 2014.

581 Lopez-Hilfiker, F. D., Mohr, C., Ehn, M., Rubach, F., Kleist, E., Wildt, J., Mentel, T. F.,
582 Carrasquillo, A. J., Daumit, K. E., Hunter, J. F., Kroll, J. H., Worsnop, D. R., and Thornton, J.
583 A.: Phase partitioning and volatility of secondary organic aerosol components formed from α-
584 pinene ozonolysis and OH oxidation: the importance of accretion products and other low
585 volatility compounds, Atmos. Chem. Phys., 15, 7765-7776, 10.5194/acp-15-7765-2015, 2015.

586 Lopez-Hilfiker, F. D., Mohr, C., D'Ambro, E. L., Lutz, A., Riedel, T. P., Gaston, C. J., Iyer, S.,
587 Zhang, Z., Gold, A., Surratt, J. D., Lee, B. H., Kurten, T., Hu, W. W., Jimenez, J., Hallquist, M.,
588 and Thornton, J. A.: Molecular Composition and Volatility of Organic Aerosol in the
589 Southeastern U.S.: Implications for IEPOX Derived SOA, Environ. Sci. Technol., 50, 2200-
590 2209, 10.1021/acs.est.5b04769, 2016.

591 Lutz, A., Mohr, C., Le Breton, M., Lopez-Hilfiker, F. D., Priestley, M., Thornton, J. A., and
592 Hallquist, M.: Gas to Particle Partitioning of Organic Acids in the Boreal Atmosphere, ACS
593 Earth Space Chem., 3, 1279-1287, 10.1021/acsearthspacechem.9b00041, 2019.

594 Mai, H., Shiraiwa, M., Flagan, R. C., and Seinfeld, J. H.: Under What Conditions Can
595 Equilibrium Gas-Particle Partitioning Be Expected to Hold in the Atmosphere?, Environ. Sci.
596 Technol., 49, 11485-11491, 10.1021/acs.est.5b02587, 2015.

https://doi.org/10.5194/amt-2022-147
Preprint. Discussion started: 28 June 2022


Atmospheric Measurement Techniques Discussions

597 Muller, M., Eichler, P., D'Anna, B., Tan, W., and Wisthaler, A.: Direct Sampling and Analysis
598 of Atmospheric Particulate Organic Matter by Proton-Transfer-Reaction Mass Spectrometry,
599 Anal. Chem., 89, 10889-10897, 10.1021/acs.analchem.7b02582, 2017.

600 Pagonis, D., Sekimoto, K., and de Gouw, J.: A Library of Proton-Transfer Reactions of H3O+
601 Ions Used for Trace Gas Detection, Journal of the American Society for Mass Spectrometry, 30,
602 1330-1335, 10.1007/s13361-019-02209-3, 2019.

603 Pankow, J. F.: AN ABSORPTION-MODEL OF THE GAS AEROSOL PARTITIONING
604 INVOLVED IN THE FORMATION OF SECONDARY ORGANIC AEROSOL, Atmos.
605 Environ., 28, 189-193, 10.1016/1352-2310(94)90094-9, 1994.

606 Pankow, J. F. and Asher, W. E.: SIMPOL.1: a simple group contribution method for predicting
607 vapor pressures and enthalpies of vaporization of multifunctional organic compounds, Atmos.
608 Chem. Phys., 8, 2773-2796, 10.5194/acp-8-2773-2008, 2008.

609 Perraud, V., Bruns, E. A., Ezell, M. J., Johnson, S. N., Yu, Y., Alexander, M. L., Zelenyuk, A.,
610 Imre, D., Chang, W. L., Dabdub, D., Pankow, J. F., and Finlayson-Pitts, B. J.: Nonequilibrium
611 atmospheric secondary organic aerosol formation and growth, Proc Natl Acad Sci U S A, 109,
612 2836-2841, 10.1073/pnas.1119909109, 2012.

613 Piel, F., Muller, M., Mikoviny, T., Pusede, S. E., and Wisthaler, A.: Airborne measurements of
614 particulate organic matter by proton-transfer-reaction mass spectrometry (PTR-MS): a pilot
615 study, Atmos. Meas. Tech., 12, 5947-5958, 10.5194/amt-12-5947-2019, 2019.

616 Piel, F., Müller, M., Winkler, K., Skytte af Sätra, J., and Wisthaler, A.: Introducing the extended
617 volatility range proton-transfer-reaction mass spectrometer (EVR PTR-MS), Atmos. Meas.

https://doi.org/10.5194/amt-2022-147
Preprint. Discussion started: 28 June 2022


Atmospheric Measurement Techniques Discussions

618 Tech., 14, 1355-1363, 10.5194/amt-14-1355-2021, 2021.

619 Sekimoto, K., Li, S. M., Yuan, B., Koss, A., Coggon, M., Warneke, C., and de Gouw, J.:
620 Calculation of the sensitivity of proton-transfer-reaction mass spectrometry (PTR-MS) for
621 organic trace gases using molecular properties, International Journal of Mass Spectrometry, 421,
622 71-94, 10.1016/j.ijms.2017.04.006, 2017.

623 Shiraiwa, M. and Seinfeld, J. H.: Equilibration timescale of atmospheric secondary organic
624 aerosol partitioning, Geophysical Research Letters, 39, n/a-n/a, 10.1029/2012gl054008, 2012.

625 Shiraiwa, M., Zuend, A., Bertram, A. K., and Seinfeld, J. H.: Gas-particle partitioning of
626 atmospheric aerosols: interplay of physical state, non-ideal mixing and morphology, Phys.
627 Chem. Chem. Phys., 15, 11441-11453, 10.1039/c3cp51595h, 2013.

628 Stark, H., Yatavelli, R. L. N., Thompson, S. L., Kang, H., Krechmer, J. E., Kimmel, J. R., Palm,
629 B. B., Hu, W. W., Hayes, P. L., Day, D. A., Campuzano-Jost, P., Canagaratna, M. R., Jayne, J.
630 T., Worsnop, D. R., and Jimenez, J. L.: Impact of Thermal Decomposition on Thermal
631 Desorption Instruments: Advantage of Thermogram Analysis for Quantifying Volatility
632 Distributions of Organic Species, Environ. Sci. Technol., 51, 8491-8500,
633 10.1021/acs.est.7b00160, 2017.

634 Tan, W., Zhu, L., Mikoviny, T., Nielsen, C. J., Wisthaler, A., Eichler, P., Muller, M., D'Anna,
635 B., Farren, N. J., Hamilton, J. F., Pettersson, J. B. C., Hallquist, M., Antonsen, S., and Stenstrom,
636 Y.: Theoretical and Experimental Study on the Reaction of tert-Butylamine with OH Radicals
637 in the Atmosphere, J. Phys. Chem. A, 122, 4470-4480, 10.1021/acs.jpca.8b01862, 2018.

638 Thompson, S. L., Yatavelli, R. L. N., Stark, H., Kimmel, J. R., Krechmer, J. E., Day, D. A., Hu,

https://doi.org/10.5194/amt-2022-147
Preprint. Discussion started: 28 June 2022

639 W., Isaacman-VanWertz, G., Yee, L., Goldstein, A. H., Khan, M. A. H., Holzinger, R., Kreisberg,
640 N., Lopez-Hilfiker, F. D., Mohr, C., Thornton, J. A., Jayne, J. T., Canagaratna, M., Worsnop, D.
641 R., and Jimenez, J. L.: Field intercomparison of the gas/particle partitioning of oxygenated
642 organics during the Southern Oxidant and Aerosol Study (SOAS) in 2013, Aerosol Sci. Technol.,
643 51, 30-56, 10.1080/02786826.2016.1254719, 2016.

644 Veres, P., Roberts, J. M., Warneke, C., Welsh-Bon, D., Zahniser, M., Herndon, S., Fall, R., and
645 de Gouw, J.: Development of negative-ion proton-transfer chemical-ionization mass
646 spectrometry (NI-PT-CIMS) for the measurement of gas-phase organic acids in the atmosphere,
647 International Journal of Mass Spectrometry, 274, 48-55, 10.1016/j.ijms.2008.04.032, 2008.

648 Voliotis, A., Wang, Y., Shao, Y., Du, M., Bannan, T. J., Percival, C. J., Pandis, S. N., Alfarra, M.
649 R., and McFiggans, G.: Exploring the composition and volatility of secondary organic aerosols
650 in mixed anthropogenic and biogenic precursor systems, Atmos. Chem. Phys., 21, 14251-14273,
651 10.5194/acp-21-14251-2021, 2021.

652 Wang, H. L., Lou, S. R., Huang, C., Qiao, L. P., Tang, X. B., Chen, C. H., Zeng, L. M., Wang,
653 Q., Zhou, M., Lu, S. H., and Yu, X. N.: Source Profiles of Volatile Organic Compounds from
654 Biomass Burning in Yangtze River Delta, China, Aerosol Air Qual. Res., 14, 818-828,
655 10.4209/aaqr.2013.05.0174, 2014.

656 Wang, M. Y., Chen, D. X., Xiao, M., Ye, Q., Stolzenburg, D., Hofbauer, V., Ye, P. L., Vogel, A.
657 L., Mauldin, R. L., Amorim, A., Baccarini, A., Baumgartner, B., Brilke, S., Dada, L., Dias, A.,
658 Duplissy, J., Finkenzeller, H., Garmash, O., He, X. C., Hoyle, C. R., Kim, C., Kvashnin, A.,
659 Lehtipalo, K., Fischer, L., Molteni, U., Petaja, T., Pospisilova, V., Quelever, L. L. J., Rissanen,

https://doi.org/10.5194/amt-2022-147
Preprint. Discussion started: 28 June 2022

660 M., Simon, M., Tauber, C., Tome, A., Wagner, A. C., Weitz, L., Volkamer, R., Winkler, P. M.,
661 Kirkby, J., Worsnop, D. R., Kulmala, M., Baltensperger, U., Dommen, J., El Haddad, I., and
662 Donahue, N. M.: Photo-oxidation of Aromatic Hydrocarbons Produces Low-Volatility Organic
663 Compounds, Environ. Sci. Technol., 54, 7911-7921, 2020a.

664 Wang, Q. Q., He, X., Zhou, M., Huang, D. D., Qiao, L. P., Zhu, S. H., Ma, Y. G., Wang, H. L.,
665 Li, L., Huang, C., Huang, X. H. H., Xu, W., Worsnop, D., Goldstein, A. H., Guo, H., and Yu, J.
666 Z.: Hourly Measurements of Organic Molecular Markers in Urban Shanghai, China: Primary
667 Organic Aerosol Source Identification and Observation of Cooking Aerosol Aging, ACS Earth
668 Space Chem., 4, 1670-1685, 2020b.

669 Yatavelli, R. L. N., Lopez-Hilfiker, F., Wargo, J. D., Kimmel, J. R., Cubison, M. J., Bertram, T.
670 H., Jimenez, J. L., Gonin, M., Worsnop, D. R., and Thornton, J. A.: A Chemical Ionization
671 High-Resolution Time-of-Flight Mass Spectrometer Coupled to a Micro Orifice Volatilization
672 Impactor (MOVI-HRToF-CIMS) for Analysis of Gas and Particle-Phase Organic Species,
673 Aerosol Sci. Technol., 46, 1313-1327, 2012.

674 Ye, C., Yuan, B., Lin, Y., Wang, Z., Hu, W., Li, T., Chen, W., Wu, C., Wang, C., Huang, S., Qi,
675 J., Wang, B., Wang, C., Song, W., Wang, X., Zheng, E., Krechmer, J. E., Ye, P., Zhang, Z., Wang,
676 X., Worsnop, D. R., and Shao, M.: Chemical characterization of oxygenated organic
677 compounds in the gas phase and particle phase using iodide CIMS with FIGAERO in urban air,
678 Atmos. Chem. Phys., 21, 8455-8478, 10.5194/acp-21-8455-2021, 2021.

679 Yuan, B., Koss, A. R., Warneke, C., Coggon, M., Sekimoto, K., and de Gouw, J. A.: Proton-
680 Transfer-Reaction Mass Spectrometry: Applications in Atmospheric Sciences, Chem. Rev., 117,

https://doi.org/10.5194/amt-2022-147
Preprint. Discussion started: 28 June 2022


Atmospheric Measurement Techniques Discussions

681 13187-13229, 10.1021/acs.chemrev.7b00325, 2017.

682 Zhang, X. and Seinfeld, J. H.: A functional group oxidation model (FGOM) for SOA formation
683 and aging, Atmos. Chem. Phys., 13, 5907-5926, 10.5194/acp-13-5907-2013, 2013.

684 Zhang, X., Dalleska, N. F., Huang, D. D., Bates, K. H., Sorooshian, A., Flagan, R. C., and
685 Seinfeld, J. H.: Time-resolved molecular characterization of organic aerosols by PILS plus
686 UPLC/ESI-Q-TOFMS, Atmos. Environ., 130, 180-189, 10.1016/j.atmosenv.2015.08.049,
687 2016a.

688 Zhang, X., Krechmer, J. E., Groessl, M., Xu, W., Graf, S., Cubison, M., Jayne, J. T., Jimenez,
689 J. L., Worsnop, D. R., and Canagaratna, M. R.: A novel framework for molecular
690 characterization of atmospherically relevant organic compounds based on collision cross
691 section and mass-to-charge ratio, Atmos. Chem. Phys., 16, 12945-12959, 10.5194/acp-16-
692 12945-2016, 2016b.

693 Zhao, Y. L., Kreisberg, N. M., Worton, D. R., Isaacman, G., Weber, R. J., Liu, S., Day, D. A.,
694 Russell, L. M., Markovic, M. Z., VandenBoer, T. C., Murphy, J. G., Hering, S. V., and Goldstein,
695 A. H.: Insights into Secondary Organic Aerosol Formation Mechanisms from Measured
696 Gas/Particle Partitioning of Specific Organic Tracer Compounds, Environ. Sci. Technol., 47,
697 3781-3787, 2013.

698 Zhu, H., Wang, H., Jing, S., Wang, Y., Cheng, T., Tao, S., Lou, S., Qiao, L., Li, L., and Chen,
699 J.: Characteristics and sources of atmospheric volatile organic compounds (VOCs) along the
700 mid-lower Yangtze River in China, Atmos. Environ., 190, 232-240,
701 10.1016/j.atmosenv.2018.07.026, 2018.

https://doi.org/10.5194/amt-2022-147
Preprint. Discussion started: 28 June 2022


Atmospheric Measurement Techniques Discussions

Zhu, S., Wang, Q., Qiao, L., Zhou, M., Wang, S., Lou, S., Huang, D., Wang, Q., Jing, S., Wang, H., Chen, C., Huang, C., and Yu, J. Z.: Tracer-based characterization of source variations of PM2.5 and organic carbon in Shanghai influenced by the COVID-19 lockdown, Faraday Discuss, 226, 112-137, 10.1039/d0fd00091d, 2021.